Measurement and Simulation of the Variation in Proton-Induced Energy Deposition in Large Silicon Diode Arrays

Christina L. Howe, *Student Member, IEEE,* Robert A. Weller, *Senior Member, IEEE,* Robert A. Reed, *Member, IEEE,* Brian D. Sierawski, *Member, IEEE,* Paul W. Marshall, *Member, IEEE,* Cheryl J. Marshall, *Member, IEEE,* Marcus H. Mendenhall, Ronald D. Schrimpf, *Fellow, IEEE,* John E. Hubbs, *Senior Member, IEEE*

***Abstract*— The proton induced charge deposition in a well characterized silicon P-i-N focal plane array is analyzed with Monte Carlo based simulations. These simulations include all physical processes, together with pile up, to accurately describe the experimental data. Simulation results reveal important high energy events not easily detected through experiment due to low statistics. The effects of each physical mechanism on the device response is shown for a single proton energy as well as a full proton space flux.**

***Index Terms*— focal plane array, pile up, energy deposited, Geant4, MRED, event rate.**

I. Introduction

HYBRID focal plane arrays (FPA) are increasingly being used in space applications because of their flexibility in infrared applications, reliability, low cost, high-density resolution, and on-chip signal processing [1]. FPAs have important applications for satellite missions such as spaceborne astronomy, Earth surveillance, star tracking, digital imaging, laser communications, etc. They are often used on satellites planned for long orbits in harsh proton environments requiring exceptional reliability when exposed to radiation. Because of their high sensitivity to noise, FPAs present a unique challenge in radiation hardness. Optical currents are small and near noise levels. So much that a single electron can produce enough charge to disrupt a signal [2]. Figure 1 shows how an optical sensor can be degraded by a solar proton event [3]. In figure 1, the image on the left captures a coronal mass ejection occurring on August 26, 2001. The image on the right shows the degradation of the optical device over an hour later due to the solar proton event. Spacecraft shielding helps mitigate incident electrons, but does not protect against protons which also deposit charge and create secondary electrons. Hybrid visible array technology is especially important due to advantages over CCD-based imagers in high proton exposure applications.

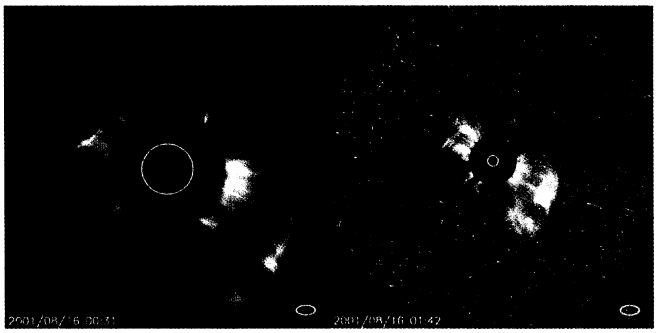

Fig. 1. Coronal mass ejection captured by LASCO on August 26, 2001. Over an hour later, degradation of the optical detector can be seen on the right figure. [3]

A better understanding of how radiation-induced energy is deposited in these devices will help lead to better prediction techniques and a greater understanding of experimental results. Accurate modeling tools will help designers better predict the on-orbit response of these increasingly popular devices. Previous Monte Carlo prediction models for these devices have shown inconsistencies with experimental data [4]. In this paper we demonstrate a high-fidelity rate-prediction approach, based on Monte Carlo simulation and a mathematical model that accounts for multiple events that affect a single pixel during the integration time. We also show that using a single-value LET and path length calculation under predicts the differential experimental spectra.

II. Experimental Description

Hybrid focal plane arrays consist of a readout integrated circuit (ROIC) and detector array fabricated separately and then joined together with interconnects such as indium columns [2]. Figure 2 shows the structure of a generic hybrid FPA. The focal plane arrays in this study are well characterized visible

Manuscript received July xxx, 2005; This work was supported in part by NASA GSFC, DTRA, MFEL Program, and MEI. The computational portion of this work was conducted through Vanderbilt Unviersity's Advanced Computing Center for Research and Education (ACCRE).

C. L. Howe is with the Department of Electrical Engineering and Computer Science, Vanderbilt University, Nashville, TN 37235 USA (email: christina.l.howe@vanderbilt.edu).

R. A. Weller, R. A. Reed, and R. D. Schrimpf are with the Department of Electrical Engineering and Computer Science and the Institute for Space and Defense Electronics, Vanderbilt University, Nashville, TN 37235 USA.

B. D. Sierawski is with the Institute for Space and Defense Electronics, Vanderbilt University, Nashville, TN 37203 USA.

P. W. Marshall is a consultant, Greenbelt, MD, 24528 USA.

C. J. Marshall is with NASA/GSFCF, Greenbelt, MD, 20771 USA.

M. H. Mendenhall is with Vanderbilt University Free Electron Laser Center, Nashville, TN 37235 USA.

J. E. Hubbs is with the Air Force Research Laboratory, Kirtland AFB, NM 87117 USA.

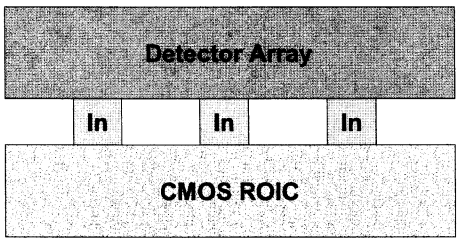

Fig. 2. A generic hybrid FPA with indium bump bonds.

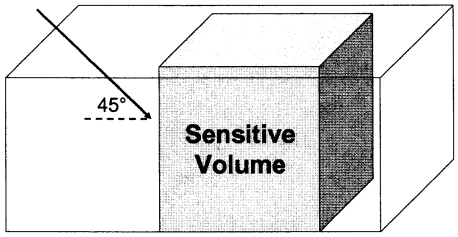

Fig. 3. Structure used to represent one pixel of a silicon p-i-n detector array. The entire structure is made of silicon and the shaded region is sensitive to the proton irradiation.

FPAs consisting of a silicon P-i-N 128 x 128 detector array with a hardened complementary metal-oxide-semiconductor (CMOS) ROIC and pixel pitch of 60 um [5]. Proton radiation studies were performed at the Crocker Nuclear Laboratory (CNL) of the University of California, Davis (UC Davis). Full radiometric characterizations were performed at each radiation dose level to determine the impact of the radiation on dark current, noise, responsivity, sensitivity, and dynamic range both pre and post radiation [5]. The total ionizing dose response of this array has been described in [5]. This paper focuses on the proton transient data, acquired at low fluxes generating sparse hits to the array with 63 MeV protons at an angle of 45 degrees. The silicon P-i-N detectors were biased to 15 volts, resulting in full depletion, and exposures were carried out at 277 K.

III. Modeling Focal Plane Array

The Monte Carlo code used in this study is MRED (Monte Carlo Radiative Energy Deposition), a GEANT4 based tool [6], [7], [8], [9], [10]. The structure used to simulate the FPA can be seen in figure 3. Sensitive region corresponds to the region in which energy deposition must occur to produce a transient event. The top and bottom of the sensitive volume are flush with the top and bottom of the surrounding material which is also silicon.

Simulations using MRED included all physics processes that are relevant for radiation effects applications, including electromagnetic and hadronic processes, and elementary particles that live long enough to be tracked. The effects of the finite integration time were simulated in a manner analogous to the computation of pile up in an ordinary nuclear spectrum. Each event in the Monte Carlo simulation represents one, and only one, primary particle. For finite integration times, there is a small but non-negligible probability of multiple hits on a single pixel (pile up). Two non-adjustable fitting parameters are used in post processing the MRED simulations. The first is μ to account for the small fraction of multiple hits and is computed by

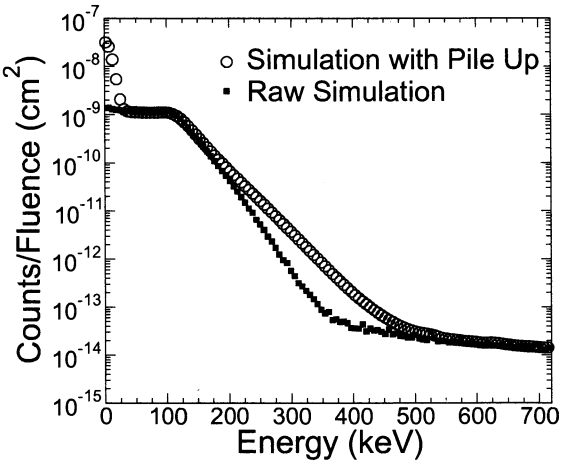

Fig. 4. MRED simulations before and after the fitting parameters for non-radiation induced noise and pile up are applied. Here μ=0.08 and σ_{noise}=3.

$$\mu = \sigma_{sim}\phi\tau_{int} \tag{1}$$

where σ_{sim} is the integral cross section of the simulation, ϕ is the experimental flux, and τ_{int} is the integration time. The second fitting parameter, σ_{noise}, is the addition of the noise observed in the experimental data and computed by

$$\sigma_{noise} = \frac{\sigma_{Gauss}}{w} \tag{2}$$

where σ_{Gauss} is the Gaussian width of the observed non-radiation induced noise in the experimental data and w is the bin width. Figure 4 compares the differential specturm of MRED simulations before and after the effects of pile up and the non-radiation induced noise were included in post-processing of the data. The shape of the sloped region between 125 and 500 keV is affected by the finite number of pixels that receive multiple hits during one integration period. The correction applied is a very general transformation of an arbitrary single-particle spectrum for the case in which the average number of hits per pixel is μ. The transformation inherently includes multiple hits of all orders, and can be used without numerical difficulty from very low fluxes well into the photon-counting region, where tens or hundreds of particles can hit a pixel in a single integration period. The region of very low energy is affected by the addition of the observed noise.

Technology computer aided design (TCAD) simulations were completed with detailed device parameters. Figure 5 shows the TCAD structure used to represent two pixels. Charge transport and collection within the device was simulated for various strike locations from a 63 MeV proton at 45 degrees. In each case, approximately 10% less charge was collected on the pixel taking the initial strike, and 10% more charge than expected was collected on the second pixel hit.

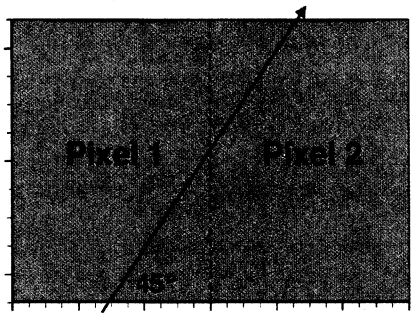

Fig. 5. TCAD structure representing two pixels. Simulations include detailed device parameters.

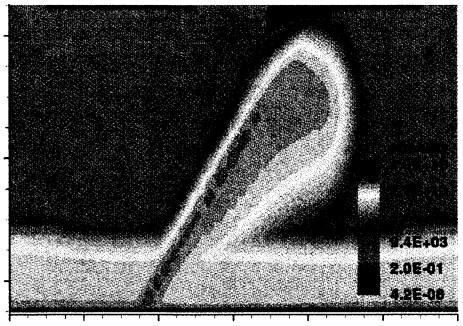

(a)

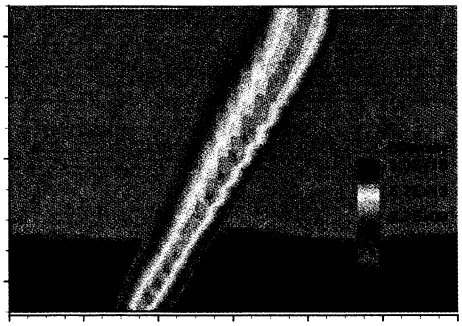

(b)

Fig. 6. (a.) Electron densiy and (b.) hole density 90 picoseconds after a strike that spans two pixels equally. The motion of charged particles is along the strike rather than vertical.

The expected collected charge was calculated using an RPP approximation. The motion of electrons and holes can be seen in figure 6. Note how the electrons and holes move along the charge strike instead of only vertically. This shows the strike can become a temporary wire causing more charge to collect on the second pixel, as noted above.

Figure 7 shows the electric field and electrostatic potential 90 picoseconds after a strike that spans two pixels equally. The slight change in electric field shows each pixel is relatively isolated from the next and then pixels behave as an rpp. From these simulations, we conclude that the rpp assumption is sufficient to estimate the device response to radiation for this technology.

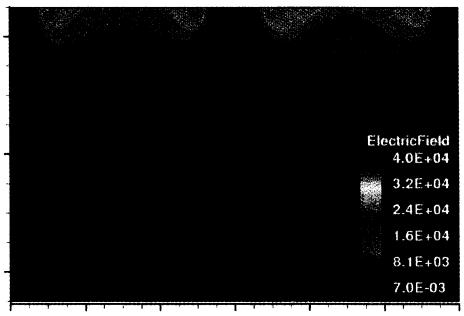

(a)

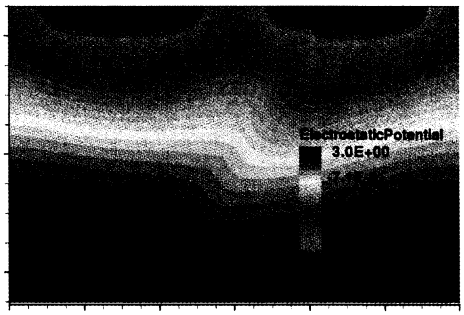

(b)

Fig. 7. (a.) Electric field and (b.) electrostatic potential 90 picoseconds after a strike that spans two pixels equally. The electric field is very slightly perturbed showing that an rpp approximation for MRED simulations is sufficient for this technology.

IV. Comparison with Experimental Data

In this section, simulated protons are incident at an angle of 45 degrees with energy of 63 MeV to match the experimental conditions. The inclusion of all physical radiation transport processes in the simulation, accounting for pile up, and the inclusion of the measured random noise spectrum provide an accurate description of the experimental data for this device with no adjustable parameters. Figure 8 shows a differential spectrum of the counts per fluence per pixel as a function of the energy deposited in the sensitive volume, comparing the experimental data with the simulation results. The conversion gain of the experimental data was extracted from the device parameters characterized during device testing. The agreement between the two curves is excellent between 0 and 300 keV. Past this region there is significant statistical uncertainty in the experimental data. Each point in the region beyond approximately 600 keV represents only one, or at most two counts. Because of the limited statistics available in test data, the higher energy events are missed during analysis of the device response. However, these high energy events will occur and could have important implications in on-orbit behavior of a device. The highest every events can give false reads on a FPA and have serious consequences during a mission so must be considered.

The dashed lines in figure 9 represent the expected average and maximum energy deposited in the structure from a constant-LET and path length distribution calculation. The dashed line labeled "Avg" is the energy deposited resulting

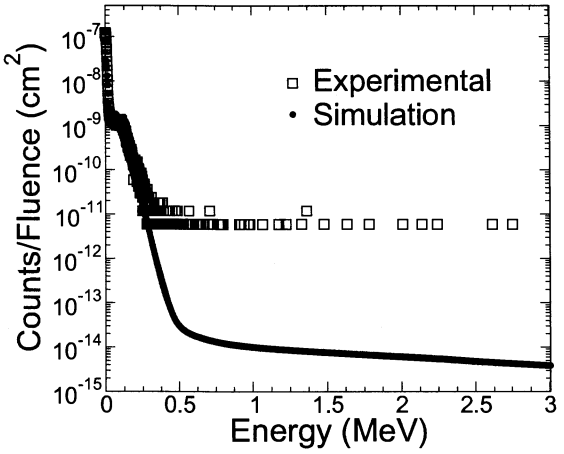

Fig. 8. Differential spectrum of counts per unit fluence per pixel for 63 MeV protons incident on the silicon detector structure from figure 3 compared with experimental results. The computed and measured total cross sections agree closely with each other and approximate the geometric cross section. The experimental data has significant statistical uncertainty at the high energy depositions.

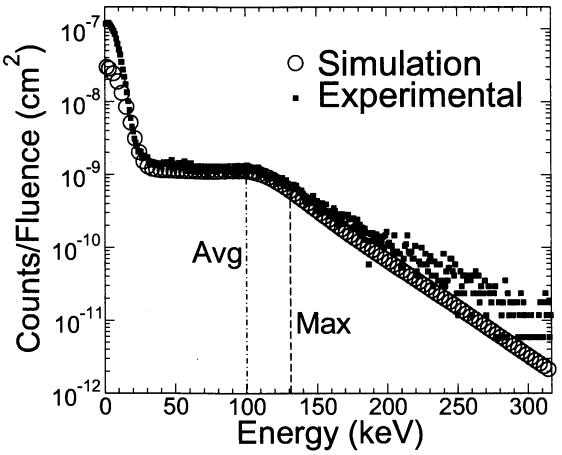

Fig. 9. Differential spectrum comparing the simulation results with experimental data and a constant LET pathlength calculation. The pathlength calculation does not predict the occurrence of large energy depositions.

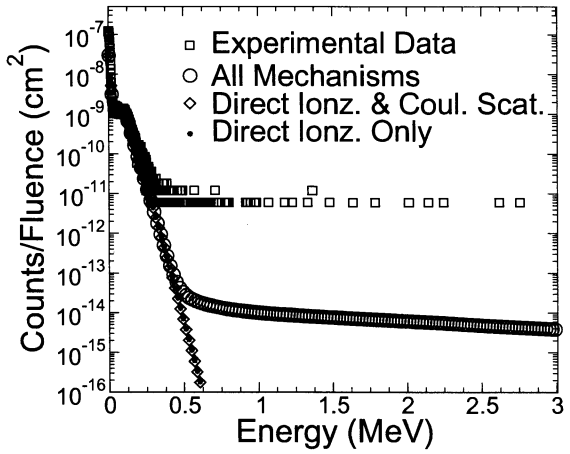

Fig. 10. Single particle MRED simulations (no pile up) comparing reaction mechanisms. The large open circles represent the simulation of all physical processes, the open diamonds include direct ionization and Coulombic scattering, and the small filled squares include only direct ionization.

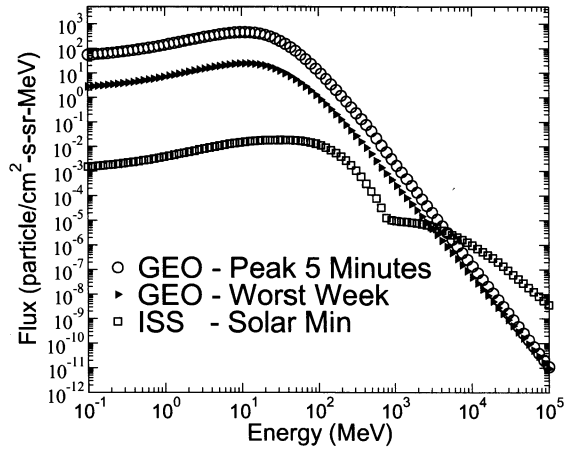

Fig. 11. Proton environments calculated using CREME [11]. The "GEO" curves are for the peak five minutes and worst week in geosynchronous orbit and "ISS" is for space station orbit using ap8min for solarmin.

from an average path length through one pixel, and the dashed line labeled "Max" is the energy deposited from a maximum path length. The maximum amount of energy deposited in the structure via this calculation is approximately 130 keV. The constant LET method predicts that no events will deposit energy greater than this value. Therefore, a constant LET does not predict the occurrence of the large energy depositions and, more interestingly, it does not describe the shape of the curve above 130 keV. Once again, the important high energy events are missed.

The simulations shown in figure 8 and 9 include primary direct ionization, Coulombic and nuclear contributions. In figure 10, we compare experimental results with MRED simulations where all processes are included, direct ionization and Coulomb scatters only, and direct ionization only. The portions of the curve visible in figure 9, the lower energy region, are largely the result of direct ionization. The constant LET approximation considers only direct ionization, but a path length analysis can only address averages while even primary ionization has fluctuations. The contribution of nuclear reactions is not significant until beyond approximately 500 keV and dominate at higher energy regions. Coulomb scatters contribute little to the cross section for this structure.

V. Modeling Energy Deposition From Space Proton FLUXES

In this section we will show event rates computed using MRED for full proton environments. For this calculation, simulations were done with an omnidirectional ion fluence. Figure 11 shows the environment models used in the calculations in this section. The curves were computed using CREME [11]. The curves labeled "GEO" are for the peak five minutes and worst week in geosynchronous orbit while the "ISS" curve represents international space station orbit using ap8min for solarmin.

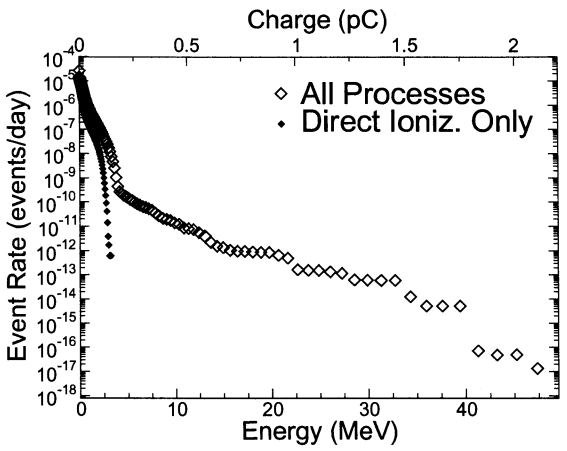

Fig. 12. Simulation results of the expected event rate from geosynchronous peak five minute and worst week proton environments in figure 11 through the pixel structure. Nuclear reactions dominate the event rate above 3 MeV (0.14 pC). *** TEMPORARY NOTE: peak 5 min. runs not complete yet ***

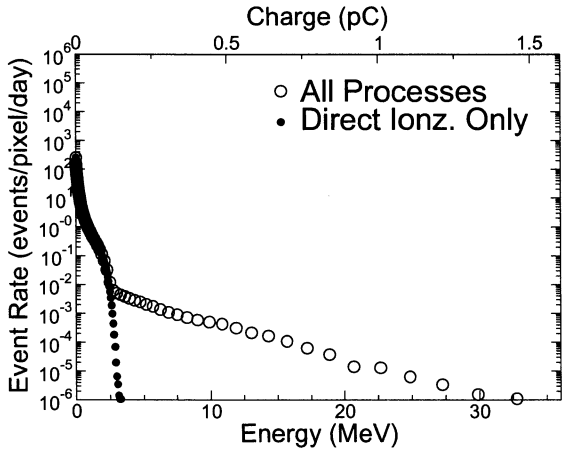

Fig. 13. Simulation results of the expected event rate from ISS orbit solar min proton environment in figure 11 through the pixel structure. The event rate is several orders of magnitude lower than the expected geosynchronous rates, but nuclear reactions still dominate the event rate above 3 MeV (0.14 pC).

Simulations shown in figure 12 compute the event rate in events per pixel per day as a function of deposited energy for the peak five minutes and worst week in the geosynchronous orbit environment. When the full proton spectra is considered, nuclear reactions dominate the event rate above an energy deposition of approximately 3 MeV (0.14 pC). When the same calculation is done for the international space station orbit, again we find above 3 MeV the rate is dominated by nuclear reactions as in figure 13. If only the direct ionization component is considered, the event rate will be underestimated.

VI. Conclusion

In this paper we show for the first time that when sufficiently complete physics is brought to bear, the results of proton irradiation of an imager can be predicted in greater detail than the resolution of the experiment reveals. The high energy events revealed through simulation are easily missed by experimental data because of low statistics. Based on test data alone, designers would be unaware of the events with the greatest potential to upset the signal. These high energy events can have serious implications on the quality of imagers used on satellites and other spacecract.

We have also shown the effects of individual mechanisms on spectral shape that can be separated and studied individually. When direct ionization only is considered, the expected on orbit cross section and event rates are underestimated. The imager described in this paper is an archetype for any silicon device, and the ability to comprehensively model radiation interactions which is an important milestone in the goal of a priori prediction of device response via Monte Carlo methods in an arbitrary radiation environment.

Acknowledgment

The computational portion of this work was conducted through Vanderbilt University's Advanced Computing Center for Research and Education (ACCRE).

References

[1] D. A. Scribner, M. R. Kruer, and J. M. Killiany, "Infrared focal plane array technology," *Proc. IEEE*, vol. 79, pp. 66–85, 1991.

[2] J. Pickel, "Novel devices and sensors," 1993 IEEE Nuclear and Space Radiation Effects Conference Short Course, Snowbird, UT, July 1993.

[3] (2007) Solar and helispheric observatory website. [Online]. Available: http://sohowww.nascom.nasa.gov

[4] S. Onoda, T. Hirao, J. S. Laird, T. Wakasa, T. Yamakawa, T. Okamoto, Y. Koizumi, and T. Kamiya, "Development of Monte Carlo modeling for proton induced charge in si pin photodiode," *IEEE Trans. Nucl. Sci.*, vol. 51, pp. 2270–2775, 2004.

[5] J. E. Hubbs, M. E. Gramer, D. C. Arrington, G. A. Dole, D. Maestas-Jepson, and S. E. Takeall, "Total ionizing dose and proton radiation characterization of si p-i-n visible hybrid focal plane arrays," *Proc. SPIE*, vol. 5902, pp. 128–142, 2005.

[6] C. L. Howe, R. A. Weller, R. A. Reed, M. H. Mendenhall, R. D. Schrimpf, K. M. Warren, D. R. Ball, L. W. Massengill, K. A. LaBel, J. W. Howard, Jr., and N. F. Haddad, "Role of heavy-ion nuclear reactions in determining on-orbit single event error rates," *IEEE Trans. Nucl. Sci.*, vol. 52, pp. 2182–2188, 2005.

[7] K. M. Warren, R. A. Weller, M. H. Mendenhall, R. A. Reed, D. R. Ball, C. L. Howe, B. D. Olson, M. L. Alles, L. W. Massengill, R. D. Schrimpf, N. F. Haddad, S. E. Doyle, D. McMorrow, J. S. Melinger, and W. T. Lotshawand, "The contribution of nuclear reactions to single event upset cross-section measurements in a high-density SEU hardened SRAM technology," *IEEE Trans. Nucl. Sci.*, vol. 52, pp. 2125–2131, 2005.

[8] A. S. Kobayashi, D. R. Ball, K. M. Warren, R. A. Reed, M. H. Mendenhall, R. D. Schrimpf, and R. A. Weller, "The effect of metallization layers on single event susceptibility," *IEEE Trans. Nucl. Sci.*, vol. 52, pp. 2189–2193, 2005.

[9] S. Agostinelli *et al.*, "Geant4-a simulation toolkit," *Nucl. Instrum. Methods Phys. Res. A*, vol. 506, pp. 250–303, 2003.

[10] M. H. Mendenhall and R. A. Weller, "An algorithm for computing screened Coulomb scattering in Geant4," *Nucl. Instrum. Methods Phys. Res. A*, vol. 227, pp. 420–430, 2005.

[11] (1997) Cosmic ray effects on micro electronics website. [Online]. Available: https://creme96.nrl.navy.mil/